

# TDDFT+ $U$ : Hubbard corrected density-functional theory in the excited-state regime

Okan K. Orhan<sup>1</sup> and David D. O'Regan<sup>1</sup>

<sup>1</sup>*School of Physics, Trinity College Dublin, Dublin 2, Ireland*

(Dated: March 16, 2017)

We develop a generalization of the density functional theory + Hubbard  $U$  (DFT+ $U$ ) method to the excited-state regime, in the form of Hubbard  $U$  corrected linear-response time-dependent DFT or ‘TDDFT+ $U$ ’. Combined with calculated linear-response Hubbard  $U$  parameters, this represents a computationally light, first-principles method for the simulation of tightly-bound excitons on transition-metal ions and more generally. In detailed calculations on closed-shell nickel coordination complexes, we find that the exchange-like Hubbard  $U$  correction to the TDDFT interaction kernel acts to substantially mitigate the excitation energy increase with  $U$  in the underlying Kohn-Sham eigenvalues. This effect is most pronounced for optically dark transitions between localized orbitals, for which experimental observation may be challenging and theoretical approaches are important. The present implementation combines linear-scaling DFT+ $U$  and linear-scaling linear-response TDDFT, but the approach is widely applicable and suited to high-throughput frameworks.

Density-functional theory (DFT) [1, 2] provides a general, computationally tractable means by which to investigate the quantum mechanically derived properties of molecules and materials. TDDFT [3] is its elegant extension of DFT to the dynamical, or excited-state regime. TDDFT is now widely used to investigate the excitation spectra of extended solids and molecules alike [4–6], due to its relatively low computational cost relative to wavefunction and Green’s function based approaches. While DFT and TDDFT are both exact in principle, their accuracies in practice are limited by the approximations currently available for the exchange-correlation (xc) contribution to the total-energy functional  $E_{xc}$  and its derived interaction kernel (by second functional derivatives)  $f_{xc}$ . Common xc-functionals include local functionals such as the local density approximation [2], semi-local functionals such as generalized gradient approximations [7], and semi-empirical functionals such as hybrids [8–10]. In practice, an adiabatic, i.e., time-averaged interaction approximation is made to construct the xc-kernels of contemporary applied TDDFT. The latter is often also restricted to the linear-response regime appropriate only to low energy, low oscillator strength excitations.

Perhaps the most thoroughly studied systematic error exhibited by approximate functionals is the delocalization [11] or many-body self-interaction error (SIE) [12], which may be defined globally, for a system with a continuously variable occupation number, as the deviation from piecewise linearity of the approximate DFT total-energy with respect to the total electron count [13]. For the integer-occupancy systems simulated more routinely, the generalized Koopman’s condition [14] gives a concise, practicable expression to the same physical condition, the non-compliance with which is, in most cases, responsible for the underestimated insulating gaps [15, 16] emblematic of practical DFT. In what follows it will be helpful to decompose SIE into two contributions. The first is an overestimation of the net self-repulsion of the electron density due to the spurious self-interaction of in-

dividual electron densities, particularly so for localized atomic orbitals, which gives rise to a positive energy-occupancy curvature, over-delocalized of densities, and inaccurate ground-state total energies. The second is the lack of any distinction between the density due to electrons already existing in a system and that due to any newly removed or added electrons, which results in the spurious absence of derivative discontinuities in the energy-occupancy curve and, consequently, the shallowing of electron removal and addition levels and the underestimation of insulating gaps. Adiabatic linear-response TDDFT inherits both components of SIE from the underlying DFT and, in this work, we address on the former.

The SIE is most problematic for systems comprising spatially localized, partially filled frontier orbitals including those of  $1s$  and  $2p$  but more canonically  $3d$  and  $4f$  character, where the qualitative failure of local functionals has been thoroughly analysed [17–20]. First-row transition metals systems thus typically require corrective measures that augment conventional closed-form density functionals, and a widely used approach at present is the computationally expedient DFT+ $U$ , which has been successfully applied to extended solids [17, 19, 21–26] and molecular systems [27–32] alike. DFT+ $U$  attains the status of a first-principles method through the direct calculation of the requisite Hubbard  $U$  parameters, and for which a number of methods have been proposed [20, 25, 32–35]. It is compatible with linear-scaling methods [36, 37] for spatially complex systems, as well as with high-throughput materials informatics approaches [38, 39]. Beginning with Ref 33, and continued in Refs. 26, 29, 30, and 40, the concept of DFT+ $U$  as a corrective method for SIE has been extensively developed, with the Hubbard  $U$  parameters playing the role of localized error quantifiers for the approximate functional [20], and we follow this interpretation here.

The effect of SIE on electron dynamics and neutral electronic excitations, such as those routinely studied using TDDFT, has attracted increasing investigation in

recent years [41–44]. It is a matter of central importance, for example, in the first-principles simulation of out-of-equilibrium nanoscale functionalities such as non-equilibrium Coulomb blockade [45, 46], and in the first-principles spectroscopy of systems comprising transition-metal ions [47–52]. Turning to non-atomistic calculations, the TDDFT solution of Hubbard type models have also attracted attention [53–56], and TDDFT has also been combined with dynamical mean-field theory for model Hamiltonians [57, 58]. Somewhat surprisingly, perhaps, given its relatively moderate computational cost and conceptual simplicity, the error correction of approximate TDDFT by means of DFT+ $U$ , in the guise of adiabatic TDDFT+ $U$  has received much less attention to date. Within its range of applicability, TDDFT+ $U$  potentially offers substantial efficiency advantages over more involved methods for calculating neutral excitations in complex transition-metal molecules and solids, such as hybrid TDDFT [59, 60], or Green’s function based methods such as GW + Bethe-Salpeter [61]. TDDFT+ $U$  is readily compatible with linear-scaling DFT, as demonstrated in the present work though the combination of linear-scaling DFT+ $U$  [36, 37] and linear-scaling TDDFT [62–64], as well as with high-throughput materials screening techniques where DFT+ $U$  is commonplace [38]. To our knowledge, the first reported TDDFT+ $U$  implementation was that of Ref. 65, combining real-time propagation and a plane-wave basis, followed by Ref. 66, which detailed the results of a linear-response implementation applied to bulk NiO. In that system, TDDFT+ $U$  was shown to be capable of reproducing the experimentally observed, tightly-bound Frenkel excitons, but not their multiplet structure, within a reasonable energy range, spectroscopic features which neither the adiabatic LDA, nor the random phase approximation built from LDA+ $U$ , succeeded in recovering to any extent. The role of DFT+ $U$  in calculated excitation energies, particularly the explicit contribution from the Hubbard term, has been explored in Ref. 67. Recently, in Ref. 68, a real-time plane-wave TDDFT+ $U$  implementation has been coupled with Ehrenfest molecular dynamics to simulate both long and short-ranged dynamical charge-transfer between alkali atom impurities and conjugated carbon systems, revealing the tendency for an increasing Hubbard  $U$  to promote the availability of multiple low-energy states in such systems, as well as to increase in energy and broaden the impurity-bath charge-transfer resonances. To date, however, information has been lacking on how the Hubbard  $U$  correction affects the typical products of practical TDDFT calculations in simple transition-metal systems, namely the low-energy excitation spectra and dipole-dipole absorption spectra, for better or worse with respect to experiment. In this Article, therefore, we systematically investigate the role of DFT+ $U$  as it individually alters the Kohn-Sham eigenspectrum underling a linear-response

TDDFT calculation, and the TDDFT interaction kernel itself. Two representative closed-shell nickel complexes were chosen for study due to their relatively simple coordination chemistry. Since their Ni 3*d* sub-shells are close to being fully filled, nominally, the dominant errors in the description of these molecules using an approximate semi-local xc-functional (here PBE) and xc-kernel (adiabatic PBE) may be assumed to derive primarily from SIE (electron delocalization) rather than static (multi-reference) correlation error [11, 15]. This is not to imply, however, that multi-reference effects are irrelevant in these systems.

Concerning ourselves only with low-energy single-particle excitations in what follows, we restrict ourselves to the linear-response regime. Here, the closed-shell TDDFT problem may be expressed in the occupied-unoccupied Kohn-Sham eigenvector product space via Casida’s equation [69, 70], which is an eigenequation for the vertical excitation frequencies  $\omega$  given by

$$\begin{pmatrix} \mathbf{A} & \mathbf{B} \\ \mathbf{B}^\dagger & \mathbf{A}^\dagger \end{pmatrix} \begin{pmatrix} \mathbf{X} \\ \mathbf{Y} \end{pmatrix} = \omega \begin{pmatrix} \mathbf{X} \\ -\mathbf{Y} \end{pmatrix}. \quad (1)$$

The Hamiltonian matrix elements  $A_{vc,v'c'} = \delta_{vv'}\delta_{cc'}(\epsilon_c - \epsilon_v) + K_{vc,v'c'}$  and  $B_{vc,v'c'} = K_{vc,c'v'}$  correspond to excitation-excitation and excitation-relaxation pairs, respectively, and the ground-state Kohn-Sham eigenvalues  $\epsilon_v$  are those of occupied valence states, while the  $\epsilon_c$  are those of unoccupied conduction states. The coupling matrix  $\mathbf{K}$  incorporates all interactions between particle-hole pairs, that is all effects beyond the many-body random-phase approximation (Fermi’s Golden Rule), and is given by the valence-conduction (*vc*) product representation

$$K_{vc,v'c'} = \iiint d\mathbf{r} d\mathbf{r}' d\mathbf{r}'' d\mathbf{r}''' \psi_v^*(\mathbf{r}) \psi_c(\mathbf{r}') \times f(\mathbf{r}, \mathbf{r}', \mathbf{r}'', \mathbf{r}''') \psi_{v'}(\mathbf{r}'') \psi_{c'}^*(\mathbf{r}'''), \quad (2)$$

of the interaction kernel  $f$ , where the  $\psi$  are Kohn-Sham eigenvectors. The kernel ordinarily comprises Hartree and xc terms only, denoted by  $\hat{f}_H$  and  $\hat{f}_{xc}$ , but if a DFT+ $U$  derived correction term  $\hat{f}_U$  is added, the resulting TDDFT+ $U$  interaction kernel is given by  $\hat{f} = \hat{f}_U + 2(\hat{f}_H + \hat{f}_{xc})$ . The underling Kohn-Sham eigensystem is also changed by  $U$ , typically. The factor of 2 is due to the sum of identical (in the closed-shell case) like and unlike-spin Hartree and xc interactions acting on a given excitation, but it does not pre-multiply  $\hat{f}_U$  if DFT+ $U$  acts explicitly only on like-spin Kohn-Sham states. The rotationally-invariant DFT+ $U$  energy functional [19, 21–24] used in this work falls into that category, and it is given, for a single SIE-afflicted subspace, by

$$E_U = \sum_{\sigma} \frac{U}{2} \sum_m \left( n_{mm}^{\sigma} - \sum_{m'} n_{mm'}^{\sigma} n_{m'm}^{\sigma} \right). \quad (3)$$

Here,  $U$  is the Hubbard parameter and  $\sigma$  indexes spin. The subspace occupancy matrix  $n_{mm'}^{\sigma} =$

$\sum_v \langle \varphi_m | \psi_v^\sigma \rangle \langle \psi_v^\sigma | \varphi_{m'} \rangle$  is typically defined terms of localized orbitals (in our calculations, orthonormal atomic nickel 3d orbitals solved in the norm-conserving pseudopotential used)  $\varphi_m$ . The interaction kernel is the second functional derivative of the energy functional with respect to the density matrix [3], and we find, denoting the density-matrix for spin  $\sigma$  by  $\rho^\sigma(\mathbf{r}, \mathbf{r}')$ , that

$$\begin{aligned} f_{UU}^{\sigma\sigma'}(\mathbf{r}, \mathbf{r}', \mathbf{r}'', \mathbf{r}''') &= \frac{\delta^2 E_U}{\delta \rho^\sigma(\mathbf{r}'', \mathbf{r}''') \delta \rho^{\sigma*}(\mathbf{r}, \mathbf{r}')} \\ &= -U \delta^{\sigma\sigma'} \varphi_m(\mathbf{r}) \varphi_{m'}^*(\mathbf{r}') \\ &\quad \times \varphi_m^*(\mathbf{r}'') \varphi_{m'}(\mathbf{r}'''). \end{aligned} \quad (4)$$

The resulting Hubbard  $U$  contribution to  $\mathbf{K}$  may be variously written, using implicit summation, as

$$\begin{aligned} K_{vc,v'c'}^U &= -U \langle \psi_v | \varphi_m \rangle \langle \varphi_{m'} | \psi_{c'} \rangle (\langle \psi_{v'} | \varphi_m \rangle \langle \varphi_{m'} | \psi_{c'} \rangle)^* \\ &= -U \langle \psi_v | \varphi_m \rangle \langle \varphi_m | \psi_{v'} \rangle \langle \psi_{c'} | \varphi_{m'} \rangle \langle \varphi_{m'} | \psi_{c'} \rangle, \end{aligned} \quad (5)$$

so that the direct term for excitation self-interaction is

$$K_{vc,vc}^U = -U \sum_{mm'} |\langle \psi_v | \varphi_m \rangle|^2 |\langle \varphi_{m'} | \psi_c \rangle|^2. \quad (6)$$

The form of  $\mathbf{K}^U$  hints at the behaviour expected of the TDDFT+ $U$  excitation spectrum as  $U$  is varied. For  $U > 0$  eV, the interaction correction due to one ( $vc$ ) pair and acting upon another is a sum over typically attractive direct Hartree and exchange-like terms. Relative to the situation that holds in hybrid-exchange TDDFT, the latter terms be expected to be more dominant over the former, since in TDDFT+ $U$  the constant pre-multiplies both types. It is instructive to examine the special case in which the projecting orbitals  $\varphi_m$  are identical to a subset of the underlying Kohn-Sham states  $\psi$ . There, the Hubbard  $U$  contributions to  $\mathbf{B}$  and  $\mathbf{A}$  reduce to

$$\begin{aligned} B^U &= K_{vc,c'v'}^U = -U \delta_{vm} \delta_{mc'} \delta_{v'm'} \delta_{m'c} = 0 \quad \text{and} \quad (7) \\ A^U &= K_{vc,v'c'}^U = -U \delta_{vm} \delta_{mv'} \delta_{c'm'} \delta_{m'c} = -U \delta_{vv'} \delta_{cc'}, \end{aligned}$$

leaving a fully diagonal contribution to the Casida Hamiltonian. If these Kohn-Sham states are also well separated from all others energetically, the effect of the Hubbard  $U$  on the underlying eigenstate differences  $\epsilon_c - \epsilon_v$  will simply be an increase by  $U$ , whereupon the effects of DFT+ $U$  and TDDFT+ $U$  fully cancel for excitations coupling states within the target subspace. While this picture is complicated by Kohn-Sham state hybridization, self-consistency, and the spillage of the localized orbitals, in practice, the TDDFT+ $U$  correction may nonetheless be expected to more strongly mix transitions between states that overlap strongly with the selected subspace, and to increase their exciton binding energy by opposing to the underlying DFT+ $U$  eigenvalue correction. However, the matrix elements of  $\mathbf{K}^U$  are quadratic in overlap integrals of the form  $\langle \psi_v | \varphi_m \rangle \langle \varphi_m | \psi_c \rangle$ , whereas the underlying Hubbard  $U$  correction to the Kohn-Sham potential comprises terms linear in such integrals, so that the

effects of the former are expected to be more spectrally focused on the target subspace than those of the latter.

The principal effects of TDDFT+ $U$  are confirmed in Fig. 1, which shows the  $U$  dependence of the coupled excitations of a toy model built from four independent-particle (Kohn-Sham type) states. These dispersionless states are two valence (indexed 1 and 2) and two conduction (3 and 4), so that the matrices  $\mathbf{A}$  and  $\mathbf{B}$  are  $4 \times 4$  real symmetric. We have chosen the states closer to the Fermi level, 2 and 3, to span an idealized DFT+ $U$  subspace, such that eigenvalue 2 (3) is lowered (raised) by  $U/2$  with respect to its uncorrected value  $\epsilon^0$ , while the energy eigenvalues of 1 and 4 remain fixed. The  $U$ -dependence of the resulting independent-particle transition energies is depicted in Fig. 1a, which emulates the first-principles DFT+ $U$  & Fermi's Golden Rule (FGR).

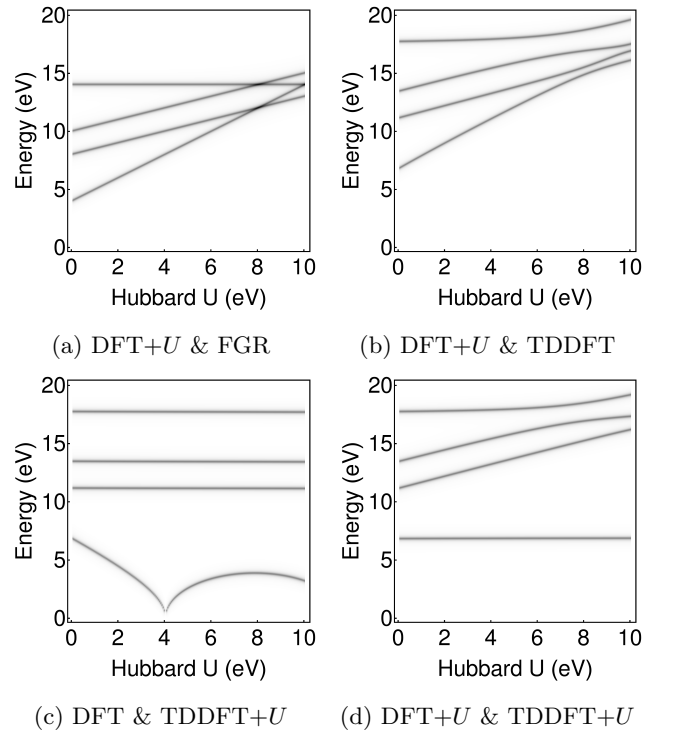


FIG. 1: Transition energies of a four-level toy model comprising two levels affected by a Hubbard  $U$  type correction, and two bystander levels, one of each type being occupied. Captions indicate the analogous DFT-based approximation, e.g., the + $U$  in ‘DFT+ $U$  & FGR’ indicates that the occupied (unoccupied) localised level is lowered (raised) by  $U/2$ , while ‘FGR’ indicates that the transitions are independent; ‘TDDFT’ denotes that a repulsive kernel (identical for all matrix elements except diagonal, which are 5 times higher) couples transitions; and ‘TDDFT+ $U$ ’ implies that the kernel is  $U$ -corrected.

The standard, Hartree + xc type TDDFT electron-hole interaction  $\mathbf{K}^0$  is set to fixed values, independent of  $U$ , of 4 eV on the diagonal and 0.8 eV on the off-diagonal,

so that  $\mathbf{B}$  is  $U$ -independent. On the other hand, the matrix elements  $A_{vc,v'c'} = \delta_{vv'}\delta_{cc'}(\epsilon_c^0 - \epsilon_v^0 + (U/2)(\delta_{c3} - \delta_{v2}) - \delta_{v2}\delta_{c3}U) + K_{vc,v'c'}^0$  incorporate DFT+ $U$  simulating  $(\pm U/2)$  and TDDFT+ $U$  simulating  $(-U)$  terms, the presence of which is indicated in the panel titles of Fig. 1. First, in Fig. 1b, which represents DFT+ $U$  & TDDFT, we see that the DFT+ $U$  eigenvalue differences are shifted upwards in energy by TDDFT for all  $U$  as a consequence of the particular  $\mathbf{K}^0$  chosen, as well exhibiting hybridization and avoided-crossing effects. Retaining the  $U$ -dependence of the interaction but not of the underlying eigenvalues, on the other hand (Fig. 1c: emulating DFT & TDDFT+ $U$ ), results in a tighter binding of the targeted  $2 \rightarrow 3$  transition with increasing  $U$ , while all other levels remain approximately unaffected, as expected. This excitation energy becomes complex (the absolute value of the frequency is shown) at  $U \approx 4$  eV, due to unphysical over-binding. Fig. 1d shows the results of combining the  $U$ -dependence of the underlying single-particle levels, emulating DFT+ $U$ , with the  $U$ -dependence in the interaction between electron-hole pairs, emulating TDDFT+ $U$ . The condition of Eqs. 7 hold precisely here, so that the two effects cancel for the  $2 \rightarrow 3$  transition, leaving it approximately  $U$ -independent in energy. The  $U$ -dependence of the target-to-bystander and bystander-to-target excitation energies is not cancelled however, and we see observe a slight modification to these energies with respect to their DFT+ $U$  & TDDFT values (Fig. 1b) due to a reduction in their hybridization with the  $2 \rightarrow 3$  transition.

We have implemented the TDDFT+ $U$  kernel of Eq. 4 in the ONETEP package [37, 71, 72]. This direct-minimization DFT code maintains a linear-scaling increase in computational expense with respect to system size, while maintaining an accuracy which is effectively equivalent to that of a plane-wave code, by expanding the Kohn-Sham density-matrix in terms of a minimal set of spatially truncated non-orthogonal generalized Wannier functions (NGWFs) which are optimized *in situ*. For calculations involving excited states, the code is capable of variationally optimizing a set of Wannier functions for the unoccupied conduction bands following the conventional total-energy minimization [73]. With this, and using the resulting joint basis of optimized valence and conduction band Wannier functions, we used the linear-scaling beyond-Tamm-Dancoff linear-response TDDFT functionality available in ONETEP [62–64], which again uses iterative minimization, as the basis for our implementation. The central element in our combination of linear-scaling TDDFT and DFT+ $U$  [37] is the *change* in DFT+ $U$  potential associated with the first-order change in Kohn-Sham density-matrix,  $\rho^{(1)}(\mathbf{r}, \mathbf{r}'; \omega)$  at a each excitation energy  $\omega$ , which is given by the same expression for both singlet and triplet excitations alike, specifically

$$v_U^{(1)}(\mathbf{r}, \mathbf{r}'; \omega) = -U \varphi_m(\mathbf{r}) \langle \varphi_m | \rho^{(1)}(\omega) | \varphi_{m'} \rangle \varphi_{m'}^*(\mathbf{r}'). \quad (8)$$

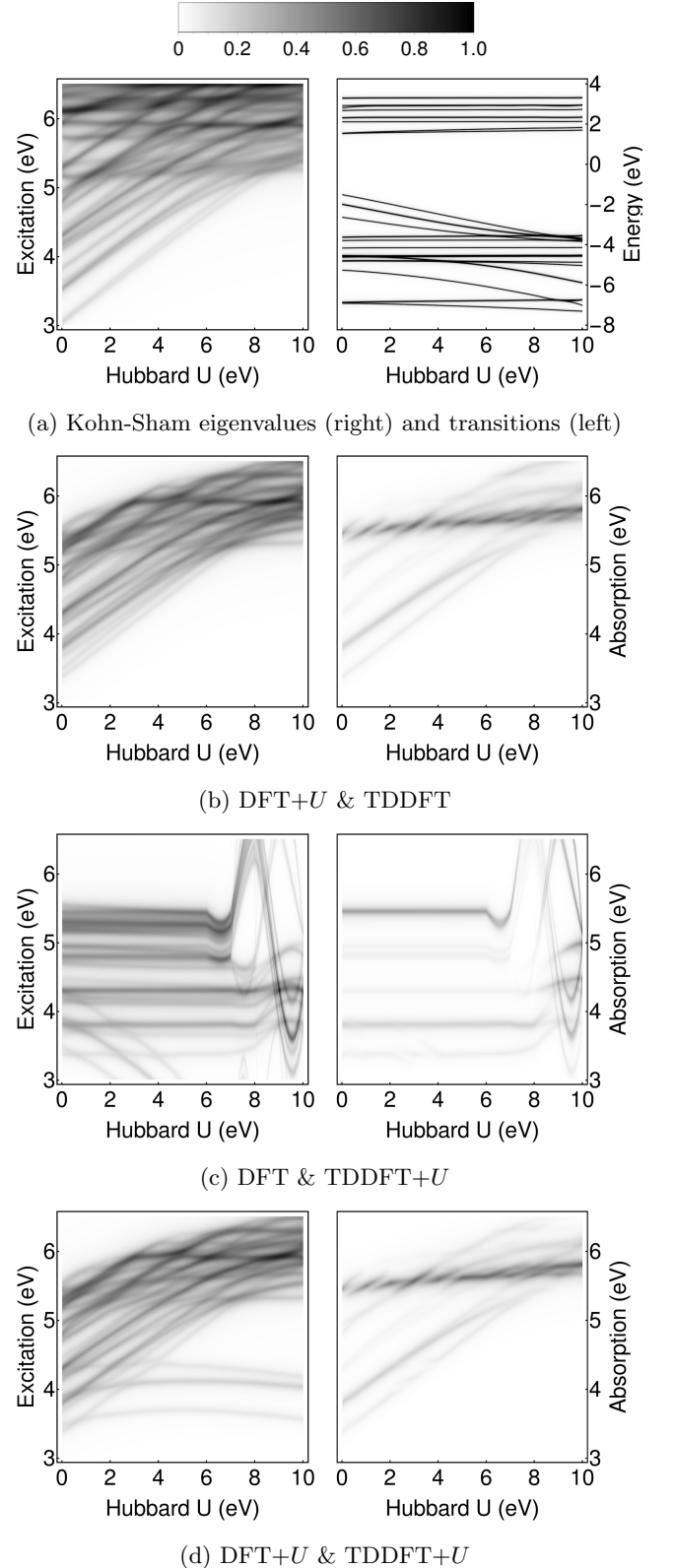


FIG. 2: The Kohn-Sham DFT eigenvalues and TDDFT excitation energies and absorption spectra of  $\text{Ni}(\text{CN})_4^{2-}$ , shown and as a function of the Hubbard  $U$  applied separately to them, with a Lorentzian broadening of 0.1 eV.



From this equation, it is clear that the occupancy dependence in the DFT+ $U$  potential survives in TDDFT+ $U$ , insofar as that, for  $U > 0$  eV, a level within the target subspace that is depopulated under excitation (typically a valence level close to the gap) will be subject to a more repulsive DFT+ $U$  potential, whereas a repopulated (conduction) level will be subject to a more attractive DFT+ $U$  potential. TDDFT+ $U$  thus tends to promote such excitations by increasing the exciton binding between the associated levels. We emphasise that the interaction in TDDFT+ $U$  remains entirely adiabatic as it is presented here, since the kernel  $f_U$  is constant, and so it addresses only the time-average of the self-interaction error as it is measured in the ground-state. As a result, it lacks the ability to produce dynamical step features in the potential as a result of occupancies passing through integer values, which is the dynamical manifestation of the second aspect of self-interaction error previously discussed. However, TDDFT+ $U$  does provide a convenient framework in which to explore non-adiabatic self-interaction correction kernels  $f_U(\omega)$ , either by means of an explicitly frequency-dependent Hubbard  $U(\omega)$ .

The effects of TDDFT+ $U$  exciton binding enhancement are illustrated in Figs. 2 and 3, which show the Hubbard  $U$  dependence of the Kohn-Sham eigenvalues, their differences, and the TDDFT single excitation spectra and electric dipole-dipole absorption spectra of two small closed-shell coordination complexes, the planar tetracyanonickelate anion  $\text{Ni}(\text{CN})_4^{2-}$  and the tetrahedral nickel tetracarbonyl  $\text{Ni}(\text{CO})_4$ . These systems enable us to explore the effects of TDDFT+ $U$  on highly-symmetric, well-studied albeit theoretically somewhat challenging singlet transitions, with a minimum of complicating factors such as periodicity and magnetism. These molecules have previously been studied experimentally [74–77] and by means of numerous first-principles methods [78–81]. In  $\text{Ni}(\text{CN})_4^{2-}$ , which is subject to the Laporte selection rule and in which the nickel atom has a nominal charge of 2+, the dominant low-lying singlet excitations are of a mixed Ni 3d  $\rightarrow$  Ni 3d and metal-to-ligand character [80]. In  $\text{Ni}(\text{CO})_4$ , these transitions are of a Ni 3d  $\rightarrow$  CO 2 $\pi^*$  type [77, 82], by virtue of a nominally fully-filled Ni 3d sub-shell. A detailed summary of how prior theoretical work has positioned bright transitions with respect to experimental peaks is provided in Tables I and II.

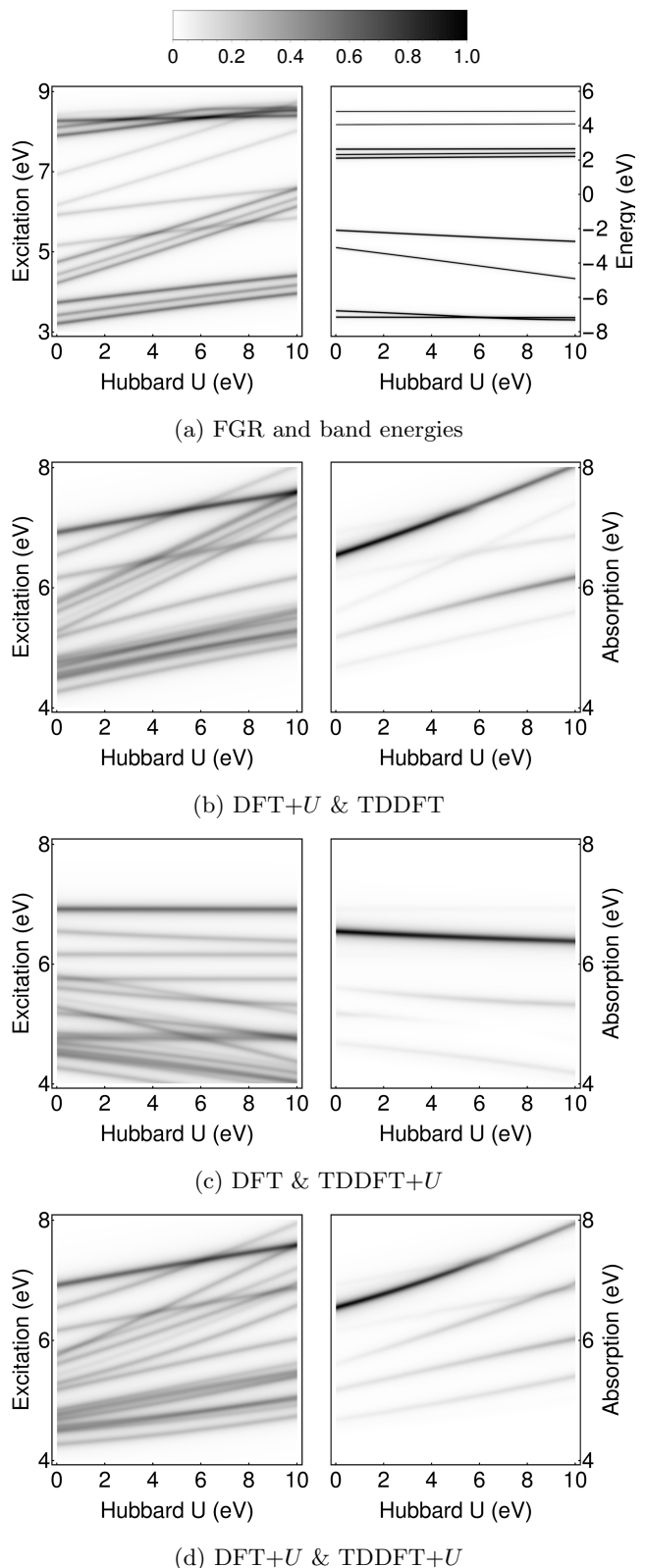


FIG. 3: The Kohn-Sham DFT eigenvalues and TDDFT excitation energies and absorption spectra of  $\text{Ni}(\text{CO})_4$ , shown and as a function of the Hubbard  $U$  applied separately to them, with a Lorentzian broadening of 0.1 eV.

In our calculations, initial molecular geometries were adopted from first-principles results [83] in the case of  $\text{Ni}(\text{CN})_4^{2-}$ , and from experimental data [84] in the case of  $\text{Ni}(\text{CO})_4$ . Convergence tests, geometry optimizations, and TDDFT calculations were performed using norm-conserving scalar-relativistic pseudopotentials (with a non-linear core correction for the Ni atom), an effective plane-wave kinetic energy cutoff of 1200 eV, and a periodic boundary correction characterized by a dimensionless cutoff parameter of 7, for which see Ref. 85. A total of 9 (18) variationally optimised nonorthogonal generalized Wannier functions were used for Ni atoms during valence (conduction) band calculations, with 4 (8) each for O, C, and N atoms. A conduction band manifold was optimized for each molecule and, in the joint basis of valence and conduction states, we optimized the first 50 singlet excitations using linear-response TDDFT.

We used a linear-response approach adapted from Ref. 20 to calculate the Hubbard  $U$  parameters for the Ni 3d orbitals from first-principles for each molecule, nothing that the DFT-derived values are those appropriate for TDDFT in the adiabatic approximation, in this case the adiabatic PBE functional. Physically plausible parameters of  $U = 1.800$  eV for  $\text{Ni}(\text{CN})_4^{2-}$  and  $U = 2.084$  eV for  $\text{Ni}(\text{CO})_4$  resulted from decoupling the spin channels in the spirit of Eq. 3. These values were used for DFT+ $U$  calculations, as well as TDDFT+ $U$  calculations either on the basis of the DFT or DFT+ $U$  ground-state Kohn-Sham eigensystem, the results of which are shown in Fig. 4 and Tables I and II. Mirroring Fig. 1, we have found it instructive to separately analyse the effects of DFT+ $U$  and TDDFT+ $U$ , which effectively compete.

The effect of DFT+ $U$  on the electronic structure of  $\text{Ni}(\text{CN})_4^{2-}$  is shown in Fig. 2a. An increasing  $U$  parameter drives the four occupied Ni 3d Kohn-Sham states near the Fermi level to lower energies. Ordered as  $E(d_{xy}) < E(d_{xz}, d_{yz}) < E(d_{z^2})$ , these appear as three due to degeneracy. The decrease in their energy increases their hybridization with the relatively unaffected bystander ligand levels. Overall, then, an increase in  $U$  leads to an increase in the low-energy excitation energies and an increase in the mixing of metal-to-ligand and ligand-to-ligand characters. This effect survives when transitions are further mixed in TDDFT, as shown in Fig. 2b, where we also note the expected splitting of excitation spectrum degeneracies and an increase in the first excitation energy with respect to DFT. Fig. 2b also shows the absorption spectrum, which is more sparse due to dipole-dipole selection but which exhibits the same principal behaviour.

The TDDFT+ $U$  kernel is switched on in Fig. 2c, but applied to the uncorrected PBE eigensystem, so that only the effect of the increasing exciton binding within the target subspace is observed. Four optically dark intra-subspace transitions to  $3d_{x^2-y^2}$  (near-degenerate with the LUMO level), are pulled down in energy rapidly with increasing  $U$ . At  $U \approx 6$  eV, ultimately, the lowest of their

energies becomes complex and the calculation becomes unreliable, reflecting the behaviour predicted by our toy model and shown in Fig. 1c. DFT+ $U$  and TDDFT+ $U$  are combined in Fig. 2d, and here we see that the effects of former prevail numerically for this system, such that singlet instability does not occur at physical  $U$  values.

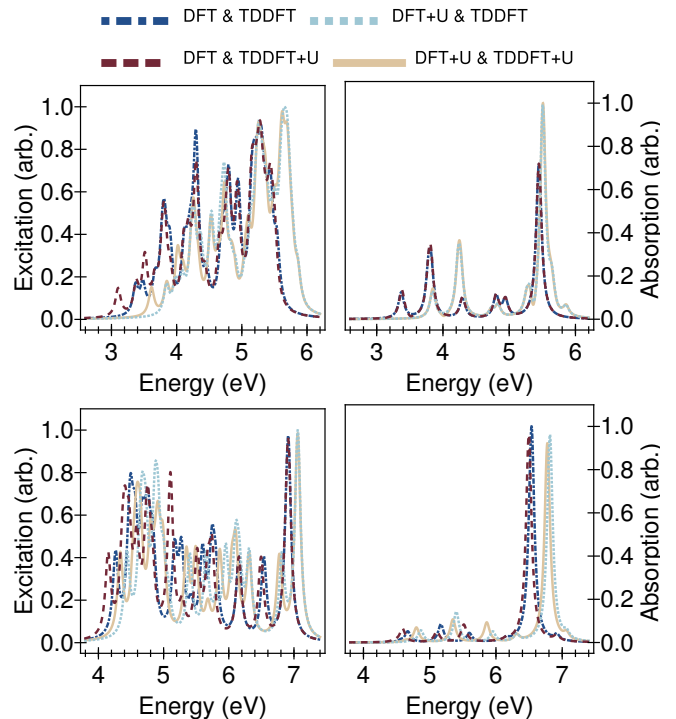


FIG. 4: The TDDFT singlet excitation and dipole-dipole absorption spectra of  $\text{Ni}(\text{CN})_4^{2-}$  (top) and  $\text{Ni}(\text{CO})_4$  (bottom), shown with a Lorentzian broadening of 0.1 eV. Hubbard  $U$  corrections were applied separately to DFT and TDDFT, as shown, using first-principles Hubbard  $U$  parameters calculated using linear-response theory.

Comparing Figs. 2b and 2d, we find that while the  $U$ -dependent optical absorption spectra is almost perfectly unaffected by the introduction of TDDFT+ $U$ , the singlet excitation spectrum paints a different picture. Beyond  $U \approx 1$  eV in DFT+ $U$  & TDDFT+ $U$  but not DFT+ $U$  & TDDFT, we observe that the lowest singlet excitation of  $\text{Ni}(\text{CN})_4^{2-}$  is an optically dark excitation localized to the Ni 3d orbitals, one which may be manifested in a plasmon in a crystalline array of a salt of this anion. Interestingly, an extremely faint absorption speak at 2.78 eV has been observed in absorption [74] and assigned a singlet character, though it has more recently been theoretically associated with a spin-forbidden transition [80]. Our results suggest the possibility, in principle, that a localised, i.e., very small oscillator strength transition either to  $3d_{x^2-y^2}$  or mixed amongst almost-filled Ni 3d orbitals (a plasmonic excitation) may be exhibited experimentally as a faint spin-allowed feature below the onset of bright metal-

to-ligand transitions. At our calculated first-principles Hubbard  $U$  parameter, this transition lies at 0.24 eV below the first bright transition, although this is very sensitive to  $U$ . We also note, considering Fig. 4 (top) for the first-principles  $U$  results, that DFT+ $U$  & TDDFT+ $U$  also predicts a strong optically dark (i.e. possibly visible by electron energy loss) feature placed approximately mid-way between the first two absorption peaks.

Method						
DFT & TDDFT (PBE)	<b>3.37</b>	3.48	<b>3.80</b>	4.13	<b>4.29</b>	<b>4.80</b>
DFT+ $U$ & TDDFT	<b>3.85</b>	3.99	4.09	<b>4.25</b>	4.36	4.53
DFT & TDDFT+ $U$	3.10	<b>3.38</b>	3.51	<b>3.80</b>	4.18	<b>4.30</b>
DFT+ $U$ & TDDFT+ $U$	3.61	<b>3.85</b>	4.02	<b>4.26</b>	4.53	<b>4.73</b>
Exp. [74]	<b>2.85</b>	<b>3.35</b>	<b>4.00</b>	<b>4.36</b>	<b>4.66</b>	-
TDDFT (PBE) [80]	<b>3.99</b>	<b>4.19</b>	<b>4.48</b>	<b>3.76</b>	<b>4.12</b>	4.53
TDDFT (LDA) [80]	<b>3.98</b>	<b>4.17</b>	<b>4.46</b>	<b>3.78</b>	<b>4.13</b>	4.55
TDDFT (B3LYP) [80]	<b>3.29</b>	<b>3.57</b>	<b>3.92</b>	<b>4.75</b>	<b>5.07</b>	5.59

TABLE I: Energies (in eV) of the singlet excitations of  $\text{Ni}(\text{CN})_4^{-2}$ , as obtained without symmetry assignment from the peak positions of Fig. 4 (top), with smaller peaks and shoulders removed. Optically bright excitations are highlighted with a bold font. Also shown are the TDDFT singlet excitations provided in Ref. 80, preserving its matching of excitations by symmetry.

The Kohn-Sham energy levels are found to be more widely separated in  $\text{Ni}(\text{CO})_4$  than in  $\text{Ni}(\text{CN})_4^{-2}$ , and so we find that DFT+ $U$  does not affect their crossing and hybridization near the Fermi level. Thus, DFT+ $U$  simply shifts the occupied bands adjacent to the Fermi level  $\text{Ni}(\text{CO})_4$  to lower energy with increasing  $U$ , as shown in Fig. 3a, thereby increasing the energies of the corresponding vertical metal-to-ligand transitions. Again, this effect is mirrored in the DFT+ $U$  & TDDFT excitation and absorption spectra shown in Fig. 3b, which shows a larger TDDFT energy increase than that observed in Fig. 2b for  $\text{Ni}(\text{CN})_4^{-2}$ . TDDFT+ $U$  again acts to enhance the intra-subspace exciton binding in  $\text{Ni}(\text{CO})_4$ , but with a less drastic effect on the excitation spectra here, since the  $3d$  sub-shell is almost fully filled. This effect may be understood in terms of the stiffening of the subspace occupancy response as subspace filling is approached, whereupon the dynamical change in the DFT+ $U$  potential is suppressed. The effect of the Hubbard  $U$  on the excitation spectrum in DFT+ $U$  & TDDFT+ $U$  (Fig. 3d) is close to the sum of the effects observed in DFT+ $U$  & TDDFT (Fig. 3b) and DFT & TDDFT+ $U$  (Fig. 3c). Overall, TDDFT+ $U$  provides a substantial mitigation of the excitation energy increase due to DFT+ $U$ , while also increasing the hybridization and avoided-crossing of transitions.

A second difference in the behaviour of TDDFT+ $U$  between  $\text{Ni}(\text{CN})_4^{-2}$  and  $\text{Ni}(\text{CO})_4$  is seen in Fig. 4, which depicts the interpolation of the spectra of Figs 2 and 3 to the

Hubbard  $U$  value calculated for each molecule. Here, we see that while TDDFT+ $U$  may shift intra-subspace transitions to lower energy in partially-filled sub-shells (top left,  $\text{Ni}(\text{CN})_4^{-2}$ ), it provides only a small rigid shift in a case of full-filling but greater hybridization (bottom left,  $\text{Ni}(\text{CO})_4$ ). We also find that the resulting effect on the absorption spectrum is negligible in a centro-symmetric molecule (top right), but that there may be some noticeable reduction in optically bright excitation energies in a molecule with no such symmetry (bottom right). Such an enhancement to the exciton binding between localized orbitals, not necessarily of  $3d$  type, is warranted in any system where a DFT+ $U$  correction to the ground-state electronic structure may be gainfully applied.

Method						
DFT & TDDFT (PBE)	4.26	4.50	<b>4.68</b>	4.75	<b>5.17</b>	5.27
DFT+ $U$ & TDDFT	4.44	4.68	<b>4.88</b>	<b>5.40</b>	5.65	<b>5.95</b>
DFT & TDDFT+ $U$	4.15	4.41	<b>4.59</b>	4.75	<b>5.10</b>	<b>5.51</b>
DFT+ $U$ & TDDFT+ $U$	4.34	4.60	<b>4.80</b>	4.91	<b>5.35</b>	5.49
Exp. (solvent) [75]	-	<b>5.24</b>	<b>5.52</b>	<b>6.02</b>	-	-
Exp. (matrix) [76]	<b>4.54</b>	<b>5.17</b>	-	-	-	-
Exp. (gas) [77]	<b>4.5</b>	<b>5.4</b>	-	-	-	-
TDDFT (LDA) [79]	<b>4.70</b>	<b>4.82</b>	<b>5.37</b>	<b>5.84</b>	<b>6.74</b>	-
SAC-CI [86]	<b>4.79</b>	<b>5.51</b>	<b>5.72</b>	<b>5.76</b>	-	-
CASPT2 [78]	<b>4.34</b>	<b>5.22</b>	<b>5.57</b>	<b>6.28</b>	<b>6.97</b>	-
TDDFT (LDA) [79]	4.36	4.60	4.62	<b>4.70</b>	<b>4.82</b>	4.95
SAC-CI [86]	4.53	4.52	4.97	<b>4.79</b>	<b>5.51</b>	6.07
CASPT2 [78]	4.04	3.58	4.88	<b>4.34</b>	<b>5.22</b>	5.15

TABLE II: Energies (in eV) of the singlet excitations of  $\text{Ni}(\text{CO})_4$ , as extracted without symmetry assignment from the peak positions of Fig. 4 (bottom), with smaller peaks and shoulders removed. Optically bright excitations are highlighted with a bold font. Also shown are the TDDFT singlet excitations provided in Ref. 79, preserving its matching of excitations by symmetry.

Previous TDDFT results are shown, with comparison to experiment following the excitation assignment provided by their respective authors, in Tables I and II. Implicit solvation with a dielectric constant of 37.5 was used in the  $\text{Ni}(\text{CN})_4^{-2}$  calculations of Ref. 80, while PBE results were not reported amongst the  $\text{Ni}(\text{CO})_4$  calculations of Ref. 79. Thus, neither set is directly comparable to our own, but they nonetheless provide a helpful benchmark. TDDFT tends to overestimate optically bright singlet transitions energies with respect to experiment in  $\text{Ni}(\text{CN})_4^{-2}$ , with our results being no exception, but the B3LYP hybrid functional was reported to perform reasonably well [80], no doubt due to its stronger exciton binding relative to LDA and PBE. The TDDFT+ $U$  kernel may be thought of as a local enhancement of exchange, so that it corrects in the same sense as hybrid

exchange. Our own vacuum TDDFT (PBE) energies fall between solvated PBE and B3LYP energies of Ref. 80. DFT+ $U$  worsens the agreement with respect to experiment, and while this is not mitigated by TDDFT+ $U$  (even slightly, by centro-symmetry), the latter does at least produce a candidate dark excitation for the weak experimental feature at 2.85 eV. In general, it is clear that in order for first-principles DFT+ $U$  and TDDFT+ $U$  to make real gains in the description of systems of this type, their exchange enhancement effect would need to apply more non-locally. For this a more appropriate population analysis, either by applying the  $U$  correction directly also to the ligands or through the use of hybridized Wannier functions [28], would be promising, as would a more flexible correction model such as DFT+ $U$ + $V$  [87], as previously applied to transition-metal chemistry [88].

TDDFT tends conversely to slightly underestimate the lowest lying bright excitation in Ni(CO)<sub>4</sub>, considering Table II. Given the relative sparsity of experimental data here, it is perhaps most appropriate to compare to high-level quantum chemistry, particularly the symmetry adapted cluster - configuration interaction (SAC-CI) results of Ref. [86]. Although the first absorption energies from SAC-CI and TDDFT+ $U$  agree very well, this is not the entire picture. With respect to the positions of the first four absorption energies from both SAC-CI and CASPT, the TDDFT+ $U$  correction does counteract an increase in the root mean square deviation caused by DFT+ $U$ , but the deviation of the uncorrected TDDFT was in both cases smaller still. TDDFT+ $U$  may therefore be most helpful for the study of neutral excitations in cases where DFT+ $U$  is necessary to obtain the correct ground-state structure in terms, e.g., of magnetic and charge ordering, particularly in systems with a size or electronic interaction strength beyond the reach of hybrid functionals. For relatively benign systems where the ground-state DFT yields a reasonable qualitative description, uncorrected TDDFT may remain more appropriate.

To summarise, we have generalised DFT+ $U$  to treat excited states involving localized, strongly interacting electrons within the framework of TDDFT. There it is readily applicable to the linear-response and full-response time-domain formalisms equally. We have applied linear-response TDDFT+ $U$ , in tandem with first-principles Hubbard  $U$  parameters, to explore the singlet excitation and optical absorption spectra of selected transition-metal coordination complexes for which theory has proven inaccurate to date, confirming the behaviour of TDDFT+ $U$  suggested by a simple four-level model. With it, we predict the presence of an optically dark singlet transition of primarily Ni  $3d_{z^2} \rightarrow 3d_{x^2-y^2}$  character in Ni(CN)<sub>4</sub><sup>2-</sup>, at an energy below the first dipole allowed transition. We have shown that the typical effect of Hubbard correction in TDDFT, more generally, will be to enhance the exciton binding among the targeted localised orbitals and in doing so, approximately but not fully, to

cancel the effect of DFT+ $U$  on the underlying Kohn-Sham eigenspectrum. TDDFT+ $U$  provides a convenient, accessible framework in which to explore dynamical strong-correlation problems such as Coulomb blockade, the spectroscopy of correlated-electron oxides, as well as the correction of approximate xc kernels for systematic errors such as many-electron self-interaction. Our implementation of TDDFT+ $U$  in the linear-scaling code ONETEP, building upon existing linear-scaling DFT+ $U$  [37] and TDDFT [62–64] functionality, opens up the possibility of Hubbard  $U$  corrected optical absorption calculations on large systems such as transition-metal doped nanoclusters, metalloproteins, and organometallic chromophores.

We gratefully acknowledge the support of Trinity College Dublin’s Studentship Award and School of Physics. The authors also acknowledge the DJEI/DES/SFI/HEA Irish Centre for High-End Computing (ICHEC) for the provision of computational facilities and support. We also acknowledge Trinity Centre for High Performance Computing and Science Foundation Ireland, for the maintenance and funding, respectively, of the Lonsdale cluster on which further calculations were performed.

- 
- [1] P. Hohenberg and W. Kohn, *Phys. Rev.* **136**, B864 (1964).
  - [2] W. Kohn and L. J. Sham, *Phys. Rev.* **140**, A1133 (1965).
  - [3] E. Runge and E. K. U. Gross, *Phys. Rev. Lett.* **52**, 997 (1984).
  - [4] M. Petersilka, U. J. Gossmann, and E. K. U. Gross, *Phys. Rev. Lett.* **76**, 1212 (1996).
  - [5] R. Bauernschmitt, M. Hser, O. Treutler, and R. Ahlrichs, *Chem. Phys. Lett.* **264**, 573 (1997).
  - [6] R. E. Stratmann, G. E. Scuseria, and M. J. Frisch, *J. Chem. Phys.* **109**, 8218 (1998).
  - [7] J. P. Perdew, K. Burke, and M. Ernzerhof, *Phys. Rev. Lett.* **77**, 3865 (1996).
  - [8] K. Kim and K. D. Jordan, *J. Phys. Chem.* **98**, 10089 (1994).
  - [9] C. Adamo and V. Barone, *J. Chem. Phys.* **110**, 6158 (1999).
  - [10] J. Heyd, G. E. Scuseria, and M. Ernzerhof, *J. Chem. Phys.* **118**, 8207 (2003).
  - [11] A. J. Cohen, P. Mori-Sánchez, and W. Yang, *Science* **321**, 792 (2008).
  - [12] J. P. Perdew and A. Zunger, *Phys. Rev. B* **23**, 5048 (1981).
  - [13] J. P. Perdew, R. G. Parr, M. Levy, and J. L. Balduz, *Phys. Rev. Lett.* **49**, 1691 (1982).
  - [14] I. Dabo, A. Ferretti, N. Poilvert, Y. Li, N. Marzari, and M. Cococcioni, *Phys. Rev. B* **82**, 115121 (2010).
  - [15] A. J. Cohen, P. Mori-Sánchez, and W. Yang, *Phys. Rev. B* **77**, 115123 (2008).
  - [16] A. J. Cohen, P. Mori-Sánchez, and W. Yang, *Chem. Rev.* **112**, 289 (2012).
  - [17] I. G. Austin and N. F. Mott, *Science* **168**, 71 (1970).
  - [18] K. Terakura, T. Oguchi, A. R. Williams, and J. Kübler, *Phys. Rev. B* **30**, 4734 (1984).



- [19] V. I. Anisimov, J. Zaanen, and O. K. Andersen, *Phys. Rev. B* **44**, 943 (1991).
- [20] M. Cococcioni and S. de Gironcoli, *Phys. Rev. B* **71**, 035105 (2005).
- [21] V. I. Anisimov, I. V. Solovyev, M. A. Korotin, M. T. Czyzyk, and G. A. Sawatzky, *Phys. Rev. B* **48**, 16929 (1993).
- [22] I. V. Solovyev, P. H. Dederichs, and V. I. Anisimov, *Phys. Rev. B* **50**, 16861 (1994).
- [23] A. I. Liechtenstein, V. I. Anisimov, and J. Zaanen, *Phys. Rev. B* **52**, R5467 (1995).
- [24] V. I. Anisimov, F. Aryasetiawan, and A. I. Liechtenstein, *J. Phys. Condens. Matter* **9**, 767 (1997).
- [25] W. E. Pickett, S. C. Erwin, and E. C. Ethridge, *Phys. Rev. B* **58**, 1201 (1998).
- [26] B. Himmetoglu, R. M. Wentzcovitch, and M. Cococcioni, *Phys. Rev. B* **84**, 115108 (2011).
- [27] D. A. Scherlis, M. Cococcioni, P. Sit, and N. Marzari, *J. Phys. Chem. B* **111**, 7384 (2007).
- [28] D. D. O'Regan, N. D. M. Hine, M. C. Payne, and A. A. Mostofi, *Phys. Rev. B* **82**, 081102 (2010).
- [29] H. J. Kulik and N. Marzari, *J. Chem. Phys* **133**, 114103 (2010).
- [30] H. J. Kulik and N. Marzari, *J. Chem. Phys* **135**, 194105 (2011).
- [31] D. J. Cole, D. D. O'Regan, and M. C. Payne, *J. Phys. Chem. Lett.* **3**, 1448 (2012).
- [32] B. Himmetoglu, A. Floris, S. de Gironcoli, and M. Cococcioni, *Int. J. Quantum Chem.* **114**, 14 (2014).
- [33] H. J. Kulik, M. Cococcioni, D. A. Scherlis, and N. Marzari, *Phys. Rev. Lett.* **97**, 103001 (2006).
- [34] F. Aryasetiawan, K. Karlsson, O. Jepsen, and U. Schönberger, *Phys. Rev. B* **74**, 125106 (2006).
- [35] E. Şaşıoğlu, C. Friedrich, and S. Blügel, *Phys. Rev. B* **83**, 121101 (2011).
- [36] M. J. Han, T. Ozaki, and J. Yu, *Phys. Rev. B* **73**, 045110 (2006).
- [37] D. D. O'Regan, N. D. M. Hine, M. C. Payne, and A. A. Mostofi, *Phys. Rev. B* **85**, 085107 (2012).
- [38] S. Curtarolo, G. L. W. Hart, M. B. Nardelli, N. Mingo, S. Sanvito, and O. Levy, *Nat. Mater.* **12**, 191 (2013).
- [39] L. A. Agapito, S. Curtarolo, and M. Buongiorno Nardelli, *Phys. Rev. X* **5**, 011006 (2015).
- [40] Q. Zhao, E. I. Ioannidis, and H. J. Kulik, *J. Chem. Phys.* **145**, 054109 (2016).
- [41] C. A. Ullrich, P.-G. Reinhard, and E. Suraud, *J. Phys. B* **31**, 1871 (1998).
- [42] J. Messud, P. M. Dinh, P.-G. Reinhard, and E. Suraud, *Phys. Rev. Lett.* **101**, 096404 (2008).
- [43] D. Hofmann, T. Körzdörfer, and S. Kümmel, *Phys. Rev. Lett.* **108**, 146401 (2012).
- [44] D. Hofmann and S. Kümmel, *J. Chem. Phys* **137**, 064117 (2012).
- [45] D. Hofmann and S. Kümmel, *Phys. Rev. B* **86**, 201109 (2012).
- [46] M. J. P. Hodgson, J. D. Ramsden, J. B. J. Chapman, P. Lillystone, and R. W. Godby, *Phys. Rev. B* **88**, 241102 (2013).
- [47] J. Autschbach, F. E. Jorge, and T. Ziegler, *Inorg. Chem.* **42**, 2867 (2003).
- [48] L. Chiodo, M. Salazar, A. H. Romero, S. Laricchia, F. D. Sala, and A. Rubio, *J. Chem. Phys* **135**, 244704 (2011).
- [49] M. Pastore, S. Fantacci, and F. De Angelis, *J. Phys. Chem. C* **117**, 3685 (2013).
- [50] E. Berardo, H.-S. Hu, H. J. J. van Dam, S. A. Shevlin, S. M. Woodley, K. Kowalski, and M. A. Zwijnenburg, *J. Chem. Theory Comput.* **10**, 5538 (2014).
- [51] E. Berardo, H.-S. Hu, S. A. Shevlin, S. M. Woodley, K. Kowalski, and M. A. Zwijnenburg, *J. Chem. Theory Comput.* **10**, 1189 (2014).
- [52] T. A. Niehaus, T. Hofbeck, and H. Yersin, *RSC Adv.* **5**, 63318 (2015).
- [53] C. Verdozzi, *Phys. Rev. Lett.* **101**, 166401 (2008).
- [54] M. Farzanehpour and I. V. Tokatly, *Phys. Rev. B* **90**, 195149 (2014).
- [55] J. I. Fuks and N. T. Maitra, *Phys. Chem. Chem. Phys.* **16**, 14504 (2014).
- [56] R. J. Magyar, *Phys. Rev. B* **79**, 195127 (2009).
- [57] D. Karlsson, A. Privitera, and C. Verdozzi, *Phys. Rev. Lett.* **106**, 116401 (2011).
- [58] S. R. Acharya, V. Turkowski, and T. S. Rahman, *Computation* **4** (2016).
- [59] P. J. Hay, *J. Phys. Chem. A* **106**, 1634 (2002).
- [60] A. Rosa, G. Ricciardi, O. Gritsenko, and E. J. Baerends, "Excitation energies of metal complexes with time-dependent density functional theory," in *Principles and Applications of Density Functional Theory in Inorganic Chemistry I* (Springer Berlin Heidelberg, Berlin, Heidelberg, 2004) pp. 49–116.
- [61] S. Körbel, P. Boulanger, I. Duchemin, X. Blase, M. A. L. Marques, and S. Botti, *J. Chem. Theory Comput.* **10**, 3934 (2014).
- [62] T. J. Zuehlsdorff, N. D. M. Hine, J. S. Spencer, N. M. Harrison, D. J. Riley, and P. D. Haynes, *J. Chem. Phys* **139**, 064104 (2013).
- [63] T. J. Zuehlsdorff, N. D. M. Hine, M. C. Payne, and P. D. Haynes, *J. Chem. Phys* **143**, 204107 (2015).
- [64] T. J. Zuehlsdorff, P. D. Haynes, F. Hanke, M. C. Payne, and N. D. M. Hine, *J. Chem. Theory Comput.* **12**, 1853 (2016).
- [65] X. Qian, D. Ceresoli, E. Li, H. J. Kulik, and N. Marzari, *APS March Meeting Abstracts* **54**, S1.097 (2009).
- [66] C.-C. Lee, H. C. Hsueh, and W. Ku, *Phys. Rev. B* **82**, 081106 (2010).
- [67] B. Himmetoglu, A. Marchenko, I. Dabo, and M. Cococcioni, *J. Chem. Phys.* **137**, 154309 (2012).
- [68] D. Shin, G. Lee, Y. Miyamoto, and N. Park, *J. Chem. Theory Comput.* **12**, 201 (2016).
- [69] M. E. Casida, in *Recent Developments and Applications of Modern Density Functional Theory*, Theoretical and Computational Chemistry, Vol. 4, edited by J. Seminario (Elsevier, 1996) pp. 391 – 439.
- [70] M. E. Casida, *Comp. Theor. Chem.* **914**, 3 (2009).
- [71] C.-K. Skylaris, P. D. Haynes, A. A. Mostofi, and M. C. Payne, *J. Chem. Phys* **122**, 084119 (2005).
- [72] P. D. Haynes, C.-K. Skylaris, A. A. Mostofi, and M. C. Payne, *physica status solidi (b)* **243**, 2489 (2006).
- [73] L. E. Ratcliff, N. D. M. Hine, and P. D. Haynes, *Phys. Rev. B* **84**, 165131 (2011).
- [74] H. B. Gray and C. J. Ballhausen, *J. Am. Chem. Soc.* **85**, 260 (1963).
- [75] A. F. Schreiner and T. L. Brown, *J. Am. Chem. Soc.* **90**, 3366 (1968).
- [76] A. B. P. Lever, G. A. Ozin, A. J. L. Hanlan, W. J. Power, and H. B. Gray, *Inorg. Chem.* **18**, 2088 (1979).
- [77] M. Kotzian, N. Roesch, H. Schroeder, and M. C. Zerner, *J. Am. Chem. Soc.* **111**, 7687 (1989).
- [78] K. Pierloot, E. Tsokos, and L. G. Vanquickenborne, *J.*

- [Phys. Chem. \*\*100\*\*, 16545 \(1996\).](#)
- [79] S. J. A. van Gisbergen, J. A. Groeneveld, A. Rosa, J. G. Snijders, and E. J. Baerends, [J. Phys. Chem. A \*\*103\*\*, 6835 \(1999\).](#)
- [80] P. Hummel, N. W. Halpern-Manners, and H. B. Gray, [Inorg. Chem. \*\*45\*\*, 7397 \(2006\).](#)
- [81] Y. Shu, E. G. Hohenstein, and B. G. Levine, [J. Chem. Phys \*\*142\*\*, 024102 \(2015\).](#)
- [82] R. G. McKinlay, N. M. S. Almeida, J. P. Coe, and M. J. Paterson, [J. Phys. Chem. A \*\*119\*\*, 10076 \(2015\).](#)
- [83] J. Demuynck, A. Veillard, and G. Vinot, [Chem. Phys. Lett. \*\*10\*\*, 522 \(1971\).](#)
- [84] L. Hedberg, T. Iijima, and K. Hedberg, [J. Chem. Phys \*\*70\*\*, 3224 \(1979\).](#)
- [85] G. J. Martyna and M. E. Tuckerman, [J. Chem. Phys. \*\*110\*\*, 2810 \(1999\).](#)
- [86] M. Hada, Y. Imai, M. Hidaka, and H. Nakatsuji, [J. Chem. Phys \*\*103\*\*, 6993 \(1995\).](#)
- [87] V. L. C. Jr and M. Cococcioni, [J. Phys. Condens. Matter \*\*22\*\*, 055602 \(2010\).](#)
- [88] H. J. Kulik and N. Marzari, [J. Chem. Phys. \*\*134\*\*, 094103 \(2011\).](#)